

Variability in link performance of an underwater acoustic network

Mandar Chitre, Iulian Topor, Rohit Bhatnagar and Venugopalan Pallayil
Acoustic Research Laboratory, Tropical Marine Science Institute,
National University of Singapore, Singapore 119227.
{mandar, iulian, rohit, venu}@arl.nus.edu.sg

Abstract—Performance prediction of underwater acoustic network protocols is difficult due to the variability of performance of individual links in the network. Link performance is usually a complex function of several environmental and modem parameters. To understand the network and link performance variability better, we deployed a 5-node network spanning an area of about 1 km² in Singapore waters over the period of a few days. We also deployed several environmental sensors to measure water currents, sea surface motion, wind speed, rain, sound speed profile, and ambient noise. Acoustic ranging between the network nodes allowed us to accurately localize the nodes underwater. By transmitting probe signals, we were able to accurately measure acoustic propagation between nodes, and understand its impact on link performance. We present preliminary results from this experiment to show how link performance varied with location, range and environmental changes.

I. INTRODUCTION

The past two decades has seen rapid progress in the area of underwater communication technology [1], [2]. As a result, there is a growing interest in exploring the use of underwater acoustic networks [3]–[5] for various sensing and monitoring applications. Performance prediction of network protocols in such networks is a difficult task, primarily because the performance of individual links in the network is highly variable. Researchers often model underwater link error rates to be some monotonic function of range; this is a crude approximation at best. Link performance is typically a complex function of many parameters including sound speed profile, seabed properties, wind-driven surface motion, bubbles, ambient noise, water currents, frequency band, modulation, receiver structure, etc. In order to gain a better understanding of network and link performance, we embarked on a series of experiments to measure communication performance along with environmental data over the period of several days at a time.

In an experiment conducted in Singapore in October 2012 (Figure 1), we deployed several networks and studied their performance over the period of about two weeks. Another similar experiment is planned in the same area for late-2013. In this paper, we present preliminary results from one of the deployments during the 2012 experiment. The deployment consisted of a 5-node network spanning an area of about 1 km² over the period of 3 days. In order to understand the variability in performance, we deployed several environmental sensors to measure water currents, sea surface motion, wind speed, rain, sound speed profile, and ambient noise. By interleaved



Fig. 1. A Unet-PANDA network node being deployed during the 2012 experiment.

transmission of carefully designed probe signals, we were able to accurately measure acoustic propagation between nodes, along with its impact on link performance. This allowed us to gain insights into how link performance varies with location, range and environmental changes.

We start by presenting an overview of our network nodes in section II. We next present details of the experimental setup in section III. This is followed by a description of the localization of the nodes in the network in section IV. In section V, we analyze the network performance and relate it to the acoustic propagation measurements as well as environmental parameters. Finally, in section VI, we summarize our findings.

II. NETWORK NODES

To allow us to rapidly deploy and recover the underwater network, we developed *Unet-PANDA* nodes that can be dropped from a boat at desired locations. Each node consists of an anchor, an underwater modem, batteries and an acoustic-release buoy (see Figure 2). When dropped, the anchor sinks to the seabed and the modem-battery-buoy assembly resides

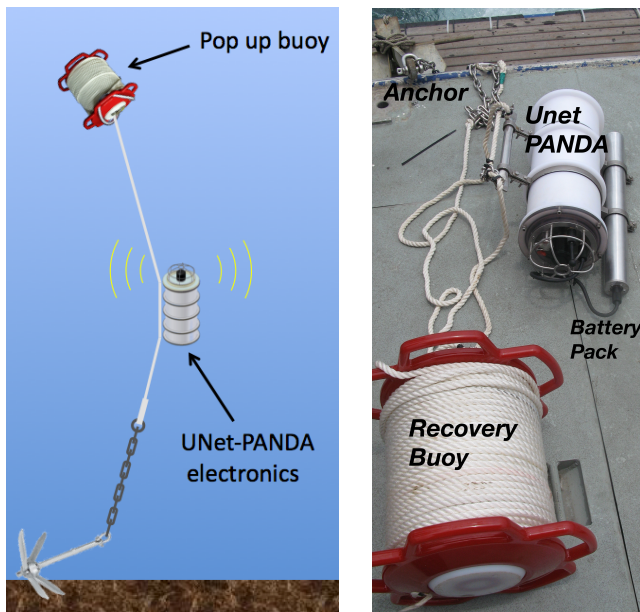


Fig. 2. Typical configuration of a Unet-PANDA network node with an anchor, electronics module and a recovery buoy. The photograph on the right shows an external battery pack attached to the Unet-PANDA, ready for deployment.

several meters above the seabed, attached to the anchor by a line. When the network is to be recovered, an acoustic command is sent to the node. This causes the buoy to surface, but remain attached to the modem-battery-anchor assembly by a line. The whole assembly is then hauled up to a boat, leaving nothing behind.

The Unet-PANDA supports internal batteries or an external battery pack. With internal batteries, the assembly is more compact but the battery capacity is limited. If longer battery life is desired, external battery pack of appropriate capacity can be mechanically attached, and connected to the Unet-PANDA through an underwater connector. During the 2012 experiment, we used external Li-ion battery packs with nominal capacity of 392 Watt-hours. The use of external battery pack enabled us to quickly swap batteries in the field, without having to wait for the internal batteries to recharge.

The external battery pack provides us an operational battery life of between 10 and 17 hours depending on the transmission duty cycle of a node. The Unet-PANDA supports a sleep-wake schedule which allowed us to use this operational battery life over a number of network tests spread over about 3 days, with each test lasting a few hours. The sleep-wake schedule is managed by a low-power STR912 micro-controller with a real-time clock (RTC). The schedule can be pre-programmed before deployment, and updated dynamically over the acoustic communication link whenever the node is awake. The RTC drift was about 4 seconds over a 3-day deployment.

The Unet-PANDA also has a GPS receiver built into it. This allows the node to know its drop location, which may be used as an initial guess of node position while determining node geometry (see section IV for details). During the 2012 experiment, the GPS functionality of the Unet-PANDA nodes

was not utilized; GPS fixes were manually taken with the deployment vessel's GPS receiver at the point of deployment.

The acoustic modem installed in the Unet-PANDA is the ARL UNET-2 modem [6]. It operates in the 18–36 kHz frequency band and has a maximum range of about 2.5 km. The modem features flexibility in the physical layer configuration with up to three distinct modulation schemes to be operated in parallel. It also features a customizable network stack with scripting capability that is invaluable for adapting test cases in the field. During the 2012 experiment, we set up the modem to use three modulation schemes: (1) an incoherent modulation scheme for a low-rate (about 400 bps after error correction) robust command link, (2) a differentially-coherent OFDM communication scheme for a higher-rate (about 5 kbps after error correction) communication link, and (3) a 500 ms long BPSK m-sequence as a probe signal for acoustic channel estimation. Each modem is installed with a USB storage device (typically 16 GB) to store network activity logs, raw acoustic recordings for each packet detected by the modem and periodic ambient noise recordings. This plethora of information allows us to investigate the acoustic propagation and noise affecting link performance during the post-experiment data analysis.

The UNET-2 modem is also equipped with an oven-controlled crystal oscillator (OCXO) for accurate timing. This can be useful in network synchronization and one-way travel-time (OWTT) acoustic ranging. Since all our network nodes during the 2012 experiments were static, two-way travel-time (TWTT) acoustic ranging could be used without loss in accuracy. To keep the battery consumption low, we disabled the OCXO during the experiment and used TWTT ranging for geometry determination.

III. EXPERIMENTAL SETUP

The 2012 experiment included multiple network deployments near Pulau Hantu, Singapore. The deployment that we will focus on in this paper lasted from 10 to 12 October 2012. The deployed network consisted of 5 nodes – 4 Unet-PANDA nodes, and 1 surface modem deployed from a barge. The locations of the nodes are shown in Figure 3. Node 21 was the surface modem deployed from the barge with a 10 m long line and 10 kg of weight. The exact depth of the modem varied depending on the prevailing currents. Nodes 22, 27, 28 and 29 were bottom-mounted Unet-PANDA nodes, each of them about 2 m off the seabed. The water depth in the area is between 7 and 20 m, typically shallow close to the islands and deeper in the middle of the channel. The seabed in the area is mostly muddy, with some sandy patches. The estimated distances between the nodes based on GPS drop locations are shown in Figure 4.

An acoustic Doppler current profiler (ADCP), a weather station (wind and rain), a video camera filming the water surface, and an underwater acoustic recording system was deployed at the barge to monitor environmental conditions. Available current and mean wind speed measurements during the deployment period are shown in Figure 5. Several conductivity-temperature-depth (CTD) profiles were obtained



Fig. 3. Five network nodes deployed in Singapore waters. Locations P21, P22, P27, P28 and P29 correspond to the drop locations of the 5 equivalently numbered nodes.

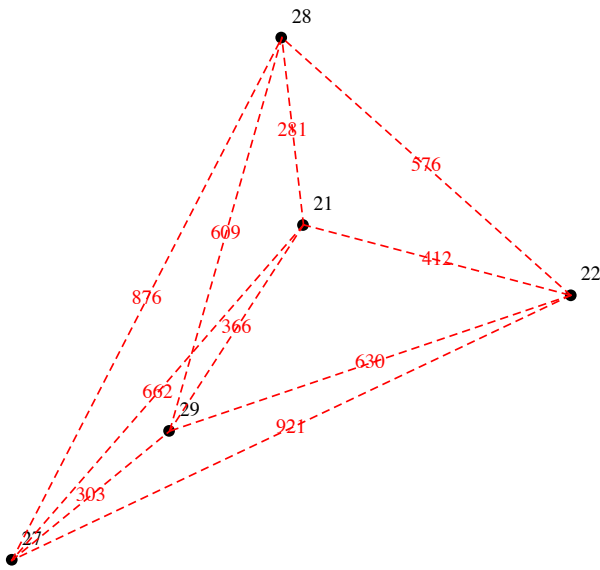
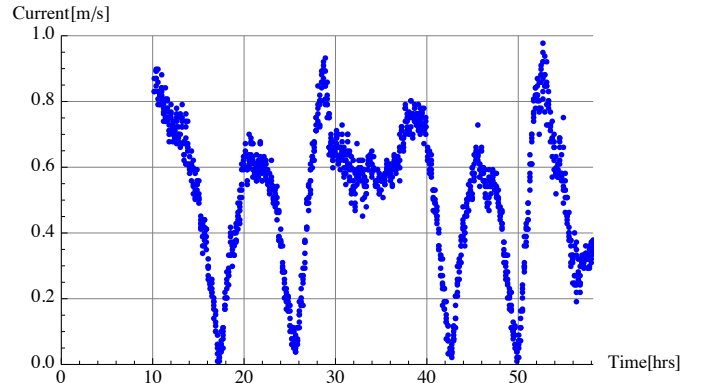


Fig. 4. Geometry of the 5-node network with nodes 21, 22, 27, 28 and 29. Estimated distances based on GPS drop locations are given in meters.

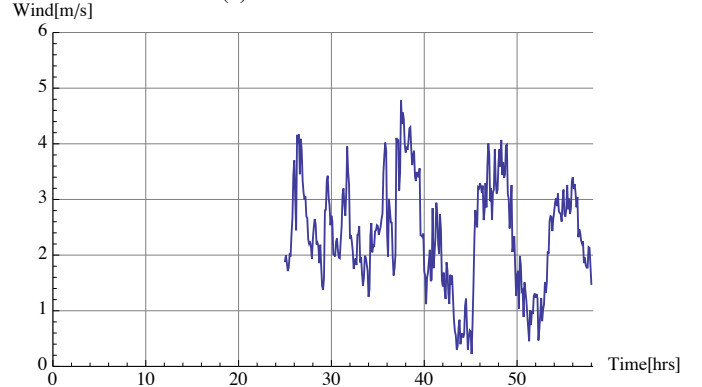
over the course of the experiment to estimate sound speed profiles. A few of the profiles are shown in Figure 6. The sound speed variation with depth and with time is very small (about 0.5 m/s). For the purpose of acoustic propagation modeling, the channel can be considered to be isovelocity.

IV. LOCALIZATION OF NETWORK NODES

After deployment of the network, an automated script was used to estimate ranges between every pair of nodes in the network using TWTT measurements. The script did not include any automated retry mechanism, so any lost packet would lead to a missing range measurement. However, the script was typically executed twice in a row to collect redundant measurements. This process was repeated periodically to track any changes in the network geometry due to limited node motion.



(a) Current measurements



(b) Mean wind speed measurements

Fig. 5. Available current and wind speed measurements at node 21 over the deployment period. The time origin is set to 00:00 on October 12, 2012.

We show one set of range measurements (in meters) made during the deployment in Table I. Where multiple measurements for a pair of nodes are available, the table shows their mean value. Cells with “-” indicate node pairs for which no measurements are available.

TABLE I
RANGE MEASUREMENTS BETWEEN NETWORK NODES

From/To	21	22	27	28	29
21	0	411.5	661.6	280.9	366.2
22	411.6	0	-	576.2	630.3
27	-	-	0	-	-
28	281.0	-	-	0	-
29	366.0	-	303.4	-	0

Let \mathbf{x}_j be the position of node $j \in \mathcal{J}$, where \mathcal{J} is the set of all nodes in the network. The range between nodes j and k is $|\mathbf{x}_j - \mathbf{x}_k|$, where $|\cdot|$ represent the Euclidean norm of the vector. Let M be the number of range measurements available, and \hat{R}_m be the range measurement between node j_m and k_m . Then the total root mean square (rms) error is given by

$$\epsilon = \sqrt{\sum_{m=1}^M \left| \hat{R}_m - |\mathbf{x}_{j_m} - \mathbf{x}_{k_m}| \right|^2}. \quad (1)$$

We may use the GPS drop locations to estimate the x and y coordinates of \mathbf{x}_j . The z coordinate can be estimated from

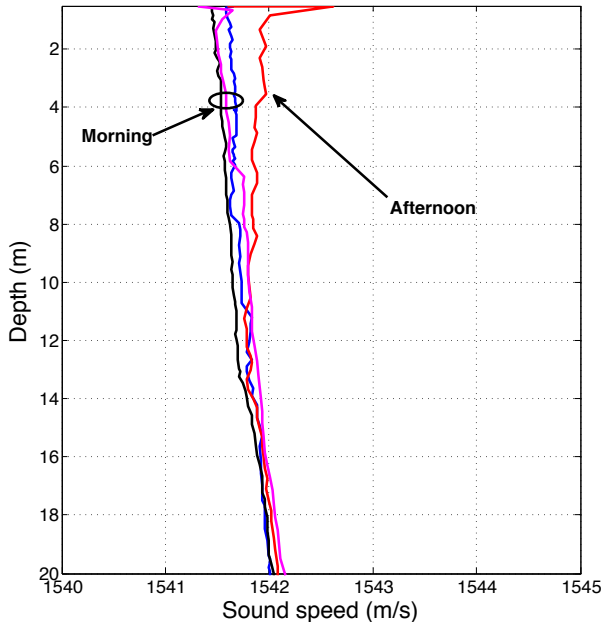


Fig. 6. CTD measurements show very little variability in sound speed as a function of depth, day or time of day. The channel can be considered approximately isovelocity.

the water depth (using the boat depth sounder) and the line length between the anchor and the Unet-PANDA electronics package. Using these \mathbf{x}_j estimates and the range measurements in Table I, we get $\epsilon = 33.4$ m. We expect that this large rms error is due to the network nodes not being at the exact location that they were dropped. With strong currents, one may expect that the nodes move up to several tens of meters before the anchors take hold into the seabed.

In order to get a better estimate of the node locations, we solve the multivariable non-linear optimization problem:

$$\{\mathbf{x}_j^*\} = \arg \min_{\{\mathbf{x}_j \forall j \in \mathcal{J}\}} \sqrt{\sum_{m=1}^M \left| \hat{R}_m - |\mathbf{x}_{j_m} - \mathbf{x}_{k_m}| \right|^2}. \quad (2)$$

We solve this problem iteratively in Mathematica (using the `FindMinimum` function) by setting the initial \mathbf{x}_j to be based on GPS and depth measurements as described above. We further constrain the problem by requiring the z coordinates of all \mathbf{x}_j to be between 0 and the maximum known depth in the area of operation, and requiring that \mathbf{x}_{21} is unchanged as node 21 is a surface node with known GPS coordinates. The resulting position estimates for the network nodes are consistent with the measurements in Table I, with an rms error $\epsilon = 0.15$ m. Figure 7 shows the estimated node locations after optimization.

For six additional range datasets obtained at other times during the deployment, we found rms error estimates of between 0.07 m and 0.85 m. We conclude that the geometry estimation procedure outlined here allows us to estimate our network node geometry to within 1 m accuracy or better.

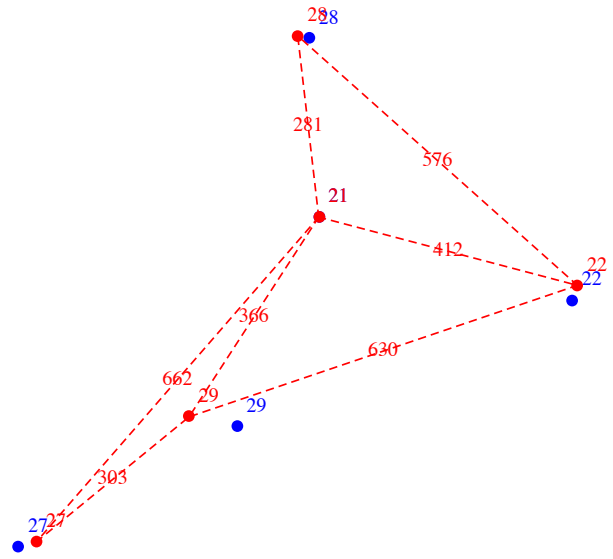


Fig. 7. Estimated geometry of the 5-node network after optimization. The isolated blue dots mark the original locations based on GPS for reference. Acoustically measured average ranges (see Table I) are shown in meters, where available.

V. DATA ANALYSIS

During the experiment, a large number of signals were transmitted by each node. These signals were received by other nodes, recorded and processed. The incoherent robust communication signals were used as a control channel to coordinate activities of the nodes. These signals are also used for link error performance analysis on all 20 links. The coherent OFDM communication signals are used to measure link performance for higher data-rate links between the nodes. The probe signals are used for acoustic propagation estimation. These signals allow us to make delay-Doppler estimates of the received signals and understand the variability in propagation.

Each signal is preceded by a 42 ms preamble that is used to detect the signal. The preamble for each of the signal type is unique, but consists of a number of overlapping linear frequency sweeps. The average signal loss rates due to missed detection are shown in Table II.

TABLE II
LOSS RATE DUE TO MISSED PREAMBLE DETECTION

From/To	21	22	27	28	29
21	-	0.047	0.095	0.026	0.056
22	0.032	-	0.228	0.139	0.081
27	0.047	0.174	-	0.025	0.011
28	0.019	0.060	0.040	-	0.420
29	0.026	0.018	0.009	0.048	-

As we can see, the probability of loss due to detection failure is quite low. However, it is interesting to note that the loss matrix is asymmetric, i.e., the probability of detection failure when node A transmits to node B, is not the same as when node B transmits to node A. The nominal source levels of each node are equal, and hence this asymmetry may be attributed to local noise conditions or non-reciprocal acoustic propagation.

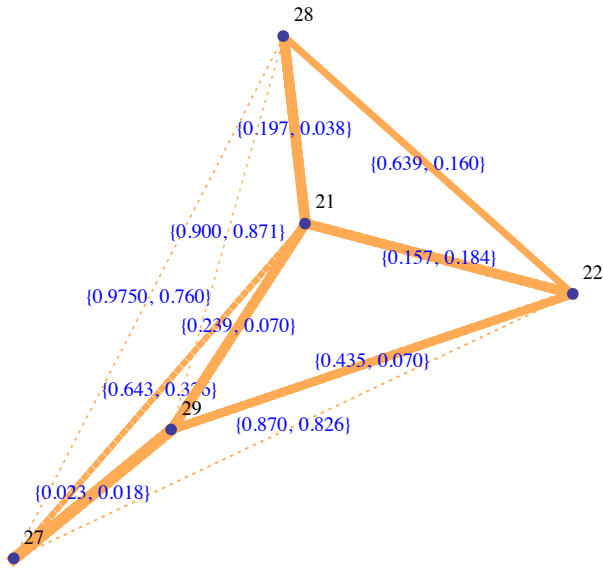


Fig. 8. Control channel packet loss rate over various network links. Thicker lines indicate better links. The values displayed on each link are packet loss rates in each of the directions, with the first value being the packet loss rate from the lower numbered node to the higher numbered node.

Noise level measurements at node 21 show variations of about 3-6 dB that are strongly correlated with the prevailing current. Other nodes showed less significant, but correlated (with current), noise variability. As node 21 was deployed in mid-water column and in the middle of the channel, we expect that it experienced the largest currents. Other nodes were close to the bottom and closer to islands/shallow areas where the current may have been weaker. Limited evidence to support this hypothesis is available from current measurements made near node 29. Nodes 28 and 29 recorded roughly 3-6 dB higher noise level than the other nodes.

Once the preamble is detected, the signal is captured and demodulated/decoded. Table III shows the control channel packet loss rate (averaged over the entire deployment) between nodes due to a combined effect of missed preamble and erroneous packet decoding. Figure 8 provides a visual representation of the same information. Nodes 28 and 29 show the strongest asymmetry in their links; this is explained by the higher noise levels at these nodes.

TABLE III
CONTROL CHANNEL PACKET LOSS RATE

From/To	21	22	27	28	29
21	-	0.157	0.643	0.197	0.239
22	0.184	-	0.870	0.639	0.435
27	0.326	0.826	-	0.975	0.023
28	0.038	0.160	0.760	-	0.900
29	0.070	0.070	0.018	0.871	-

So far, we have analyzed network link performance averaged over the entire deployment. Next, we turn our attention to variability in link performance as a function of time (and consequent environmental changes). To illustrate our key findings, we focus on a representative link between nodes 21

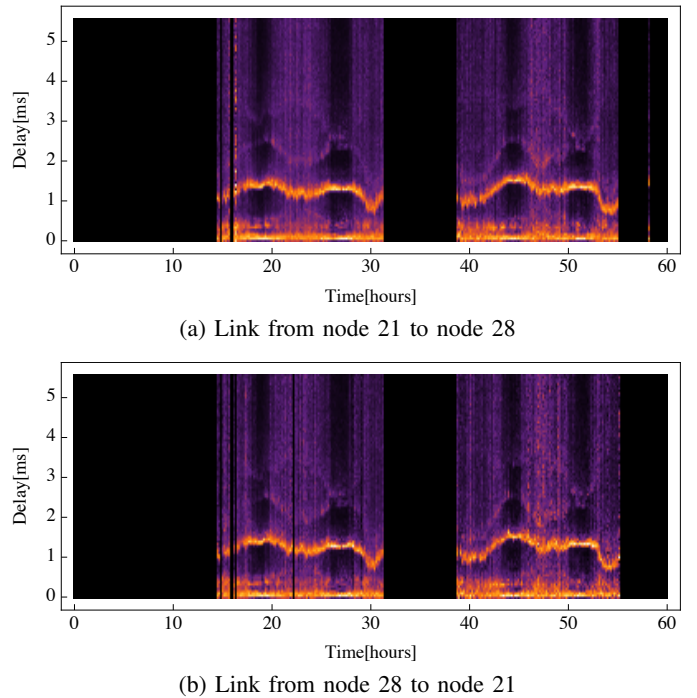


Fig. 9. Estimated impulse response for the bidirectional link between nodes 21 and 28. The impulse response shows a strong reciprocity and slow time variability.

and 28. Bidirectional impulse responses for this link are shown in Figure 9. The impulse response shows a strong reciprocity and slow time variability. Similar results are obtained for other links. Some of the links shows strong arrivals up to 10 ms delay.

Figure 10 shows the performance of the link from node 21 to 28 as a function of time. As we can see, the packet success rate of the link varies over time. However, there is no obvious correlation between the impulse response in Figure 9(a) and the packet success rate in Figure 10. It is clearly not the impulse response of the link that is the cause for packet loss. Looking at the environmental measurements in Figure 5, the currents seem to be fairly correlated with performance, while the wind does not seem to play a big role. When the current increases, the success rate drops.

The obvious candidates for affecting performance in strong currents are flow noise and Doppler. We previously noted a 3-6 dB increase in noise level during high current times. However reduction in power level by 3-6 dB during low current times did not produce the same effect, so although noise may be a contributor, it was unlikely to be the primary cause of packet loss. The control channel in the modem is routinely used for communication with autonomous underwater vehicles (AUVs) when they are moving at significantly higher speeds. Hence a constant Doppler is unlikely to be responsible for the packet loss either. In an effort to understand why the current has such a strong influence on link performance, we perform a delay-Doppler analysis on the probe signals recorded on the link from node 21 to 28. Figure 11 shows delay-Doppler

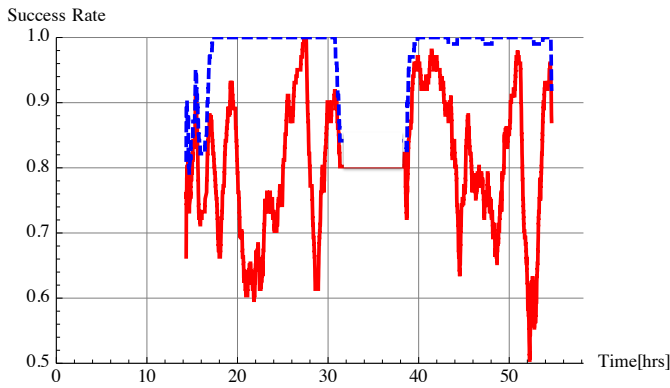


Fig. 10. Performance of link from node 21 to 28. The blue dashed line represents the packet detection rate while the red solid line represents the packet success rate.

analysis from two probe signals sent 5 seconds apart, at a time when the link performance is poor. The top panel shows a 5 Hz mean Doppler with a large spread. The bottom panel shows a -4 Hz mean Doppler with a large spread. The delay structure remains fairly stable in time over short periods, but the Doppler varies rapidly and shows a large spread. Using shorter probe signal sections for analysis, we can show that the large Doppler spread is primarily due to change in Doppler over the duration of the received signal. Figure 12 shows a delay-Doppler analysis from a probe signals at a time when the link performance is good. The Doppler spread is much lesser, and does not vary much over time. This pattern is consistent across all the data we analyzed. From this analysis, we conclude that it is the rapidly varying Doppler during high current that adversely affects the link performance.

The Doppler variability on links between two bottom-mounted nodes is significantly lower, as compared to links with the surface node. This is consistent with our belief that the current experienced by the bottom-mounted nodes is lower as compared to the surface node deployed at mid-water column in the middle of the channel. We believe that the rapid change in Doppler on our network nodes is a result of vortex-induced vibrations (VIV) [7] as a result of the current flow around the nodes. The cylindrical enclosure used to contain the electronics of each node quite likely sheds a Kármán vortex street [8] that causes the modem transducer to vibrate rapidly. As a result the transmitted and received signals experience a rapid time-varying Doppler that is detrimental to link performance.

VI. CONCLUSIONS

Link performance measurements, along with environmental data collection, over a 3-day deployment allowed us to understand the variability in communication performance as a function of environmental parameters. We found that the key parameter that affected link performance in this experiment was the current velocity. Further investigation suggests that the impact on link performance was primarily due to VIV as a result of the flow around the network node. A secondary cause of reduced performance was increase in noise level due

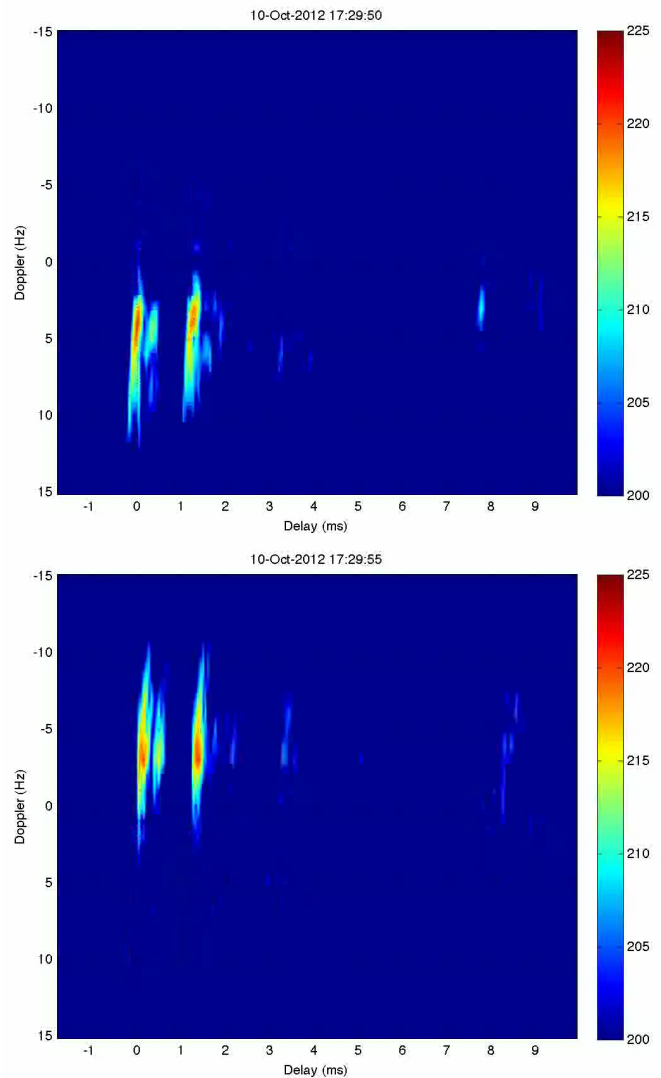


Fig. 11. Delay-Doppler analysis of probe signals sent 5 seconds apart on link from node 21 to 28 when the link performance is poor. The channel does not change much in the delay domain between the two probes, but shows a drastic change in the Doppler domain.

to currents. Designing node enclosures that reduces VIV and flow noise may lead to significant improvements in network performance.

ACKNOWLEDGMENTS

Ms. Tan Soo Pieng, Mr. Mohan Panayamadam, Mr. Harold Tay and Ms. Ang Yen Khim helped in the development and testing of the Unet-PANDA system. Dr. Matthew Legg developed the ambient noise recording system that was used during the experiment. Mr. Mohan Panayamadam, Ms. Bhavya P.H. and the Galaxea boat crew provided invaluable support during the experiment. The authors wish to express their appreciation and gratitude to all of these contributors.

REFERENCES

- [1] M. Chitre, S. Shahabudeen, and M. Stojanovic, "Underwater acoustic communications and networking: Recent advances and future challenges,"

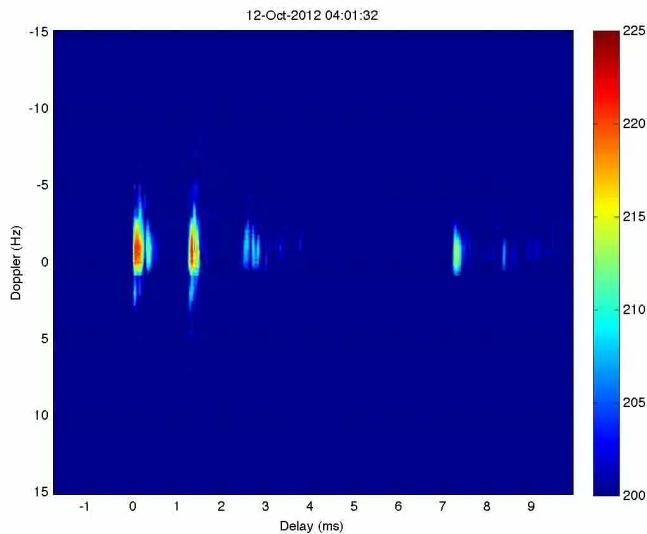


Fig. 12. Delay-Doppler analysis of a probe signal sent on link from node 21 to 28 when the link performance is good.

- The Spring 2008 MTS Journal, "The State of Technology in 2008",* vol. 42, no. 1, pp. 103–116, 2008.
- [2] A. Baggeroer, "An overview of acoustic communications from 2000-2012," in *Proceedings of Underwater Communications: Channel Modelling & Validation*, 2012.
- [3] J. Rice, "Seaweb acoustic communication and navigation networks," in *Proceedings of the International Conference on Underwater Acoustic Measurements: Technologies and Results*, 2005.
- [4] I. Akyildiz, D. Pompili, and T. Melodia, "Underwater acoustic sensor networks: research challenges," *Ad hoc networks*, vol. 3, no. 3, pp. 257–279, 2005.
- [5] J. Heidemann, W. Ye, J. Wills, A. Syed, and Y. Li, "Research challenges and applications for underwater sensor networking," in *Wireless Communications and Networking Conference, 2006. WCNC 2006. IEEE*, vol. 1. IEEE, 2006, pp. 228–235.
- [6] M. Chitre, I. Topor, and T.-B. Koay, "The UNET-2 modem – an extensible tool for underwater networking research," in *Proceedings of IEEE OCEANS'12 Yeosu*, May 2012.
- [7] R. D. Blevins, *Flow-induced vibration*. New York, NY (USA); Van Nostrand Reinhold Co., Inc., 1990.
- [8] M. Zdravkovich, "Smoke observations of the formation of a karman vortex street," *Journal of Fluid Mechanics*, vol. 37, no. 03, pp. 491–496, 1969.